

Lewis Acid Stabilized OPI_3 : Implications for the Nature of Free OPI_3 Marcin Gonsior,^[a] Lutz Müller,^[b] and Ingo Krossing*^[b, c]

Abstract: While reinvestigating the published synthesis of OPI_3 , it became evident from the experiments that phosphoryl triiodide may only be formed as an intermediate and that the end products of the reaction of OPCl_3 with LiI are P^{V} oxides, PI_3 , I_2 , and LiCl . This is also in agreement with MP2/TZVPP calculations, which assign $\Delta_r H^\circ$ ($\Delta_r G^\circ$) [$\Delta_r G^\circ$ in CHCl_3] for the disproportionation of OPI_3 as -7 (-18) [-17 kJ mol^{-1}] (assuming P_4O_{10} as the P^{V} oxide). The first products of this reaction visible in a low-temperature in

situ ^{31}P NMR experiment are P_2I_4 and PI_3 , as well as traces of a compound that may be OPCl_2I . By contrast, it was possible to prepare and structurally characterize Lewis acid [A] stabilized $[\text{A}]\leftarrow\text{OPX}_3$ adducts, where [A] is $\text{Al}(\text{OR}^{\text{F}})_3$ for $\text{X}=\text{Br}$ and $\text{Al}(\text{OR}^{\text{F}})_2(\mu\text{-F})\text{Al}(\text{OR}^{\text{F}})_3$ for $\text{X}=\text{I}$ ($\text{R}^{\text{F}}=\text{C}(\text{CF}_3)_3$). These adducts are formed on decompo-

sition of $\text{PX}_4^+[\text{Al}(\text{OR}^{\text{F}})_4]^-$; high yields of $\text{Br}_3\text{PO}\rightarrow\text{Al}(\text{OR}^{\text{F}})_3$ ($\delta(^{31}\text{P})=-65$) were obtained, while $\text{I}_3\text{PO}\rightarrow\text{Al}(\text{OR}^{\text{F}})_3$ ($\delta(^{31}\text{P})=-337$) and $\text{I}_3\text{PO}\rightarrow\text{Al}(\text{OR}^{\text{F}})_2(\mu\text{-F})\text{Al}(\text{OR}^{\text{F}})_3$ ($\delta(^{31}\text{P})=-332$) are only formed as by-products. The main product of the room-temperature decomposition of $\text{PI}_4^+[\text{Al}(\text{OR}^{\text{F}})_4]^-$ is $\text{PI}_4^+[(\text{R}^{\text{F}}\text{O})_3\text{Al}(\mu\text{-F})\text{Al}(\text{OR}^{\text{F}})_3]^-$, which was also characterized by X-ray crystallography and was independently prepared from $\text{Ag}^+[(\text{R}^{\text{F}}\text{O})_3\text{Al}(\mu\text{-F})\text{Al}(\text{OR}^{\text{F}})_3]^-$, PI_3 , and I_2 .

Keywords: ab initio calculations • donor–acceptor systems • iodine • phosphorus

Introduction

Although the synthesis of OPI_3 was already claimed in 1973^[1] and is included in every inorganic chemistry textbook, this compound is not well characterized. The original report only gives a melting point (53°C). In a CAS Online search with SCIFINDER in summer 2005 only eight references were found that contained information about OPI_3 . The only reported IR/Raman frequency of OPI_3 is the O–P stretching frequency in the gas phase at 480°C ,^[2] a temperature at which OPI_3 should already have decomposed.^[3] In

agreement with this notion, this assignment (and those of a large number of related compounds) has been questioned on the basis of quantum-chemical calculations of IR frequencies.^[4] Two of the articles on OPI_3 only include estimated thermochemical and physical properties of several oxyhalides including OPI_3 .^[5,6] No ^{31}P NMR data, conclusive vibrational spectra, or a structural report on I_3PO was given. This also includes Lewis acid stabilized species. Only $\text{I}_3\text{PO}\rightarrow\text{NbI}_5$ was briefly mentioned in a patent without any structural evidence or other method of characterization.^[7] Similarly, SPI_3 was claimed in 1964^[8] with only little characterization; later it proved impossible to verify this finding by ^{31}P NMR spectroscopy, and it was suggested that the highest possible degree of iodination is SPBrI_2 or SPClI_2 , while SPI_3 appears to decompose instantaneously with formation of lower phosphorus iodides, phosphorus sulfides, and elemental iodine.^[9] In agreement with the apparent instability of $\text{P}^{\text{V}}\text{-I}$ bonds, it was shown that P_4O_6 reacts with Cl_2 and Br_2 to give OPX_3 ($\text{X}=\text{Cl}, \text{Br}$) but with I_2 to give P_2I_4 . Oxidation of PI_3 with O_2 never gave OPI_3 .^[10] Given all these doubts it appears strange that OPI_3 is included as a “compound in a bottle” in inorganic textbooks.

Here we present the results of our attempts to repeat the syntheses of free OPI_3 , which led to the conclusion that free OPI_3 may only be present as an intermediate, even when mild conditions and low temperatures (-78°C) are used

[a] Dr. M. Gonsior
Universität Karlsruhe (TH)
Institut für Anorganische Chemie
Engesserstrasse Geb. 30.45, 76128 Karlsruhe (Germany)

[b] Dipl.-Chem. L. Müller, Prof. I. Krossing
École Polytechnique Fédérale de Lausanne (EPFL)
Laboratory of Inorganic and Coordination Chemistry
ISIC-BCH, 1015 Lausanne (Switzerland)

[c] Prof. I. Krossing
New address:
Institut für Anorganische und Analytische Chemie
Albert-Ludwigs-Universität
Albertstrasse 21, 79104 Freiburg (Germany)
E-mail: krossing@uni-freiburg.de

Supporting information for this article is available on the WWW under <http://www.chemeurj.org/> or from the author.

throughout its preparation. The final products of the reaction between OPCl_3 and LiI were identified. Subsequently we prepared and characterized Lewis acid stabilized OPX_3 ($X = \text{Br}, \text{I}$) adducts with the very strong Lewis acids $\text{Al}(\text{OR}^{\text{F}})_3$ and $\text{Al}(\text{OR}^{\text{F}})_2(\mu\text{-F})\text{Al}(\text{OR}^{\text{F}})_3$ ($\text{R}^{\text{F}} = \text{C}(\text{CF}_3)_3$). This is the first report of a molecule containing I_3PO in the solid state. Complexed I_3PO is the last missing member in the series of OPX_3 compounds ($X = \text{F}, \text{Cl}, \text{Br}, \text{I}$).

Results and Discussion

Synthesis and NMR spectroscopy

Free OPI_3 : OPI_3 was claimed^[1] to be prepared by the action of LiI on OPCl_3 or by treating PhOPI_2 with I_2 , which yielded OPI_3 and PhI . However, a more recent report on the action of LiI on SPBr_3 showed that in this case full substitution could not be achieved, and the highest iodine content observed was that in SPBrI_2 with an unusually low-frequency ^{31}P NMR signal of $\delta = -315$ ppm.^[9] The same authors extrapolated the ^{31}P NMR shift of SPI_3 to occur at $\delta \approx -411 \pm 5$ ppm. A similarly unusual ^{31}P NMR signal would be expected for free OPI_3 .

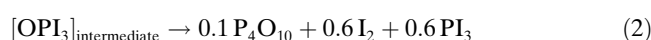
The cited melting point of OPI_3 of 53°C is close to that of PI_3 (61°C), and the observed violet color may be due to a mixture of PI_3 (red) and iodine (dark violet, m.p. 114°C). Moreover PI_3 yields the same products of hydrolysis as OPI_3 , which gave HI , H_3PO_4 , and H_3PO_3 .^[1] Therefore, we suspected that the obtained product was in fact a mixture. Free OPI_3 should not be stable under the conditions employed and would disproportionate to give phosphorus iodides and oxides, as well as elemental iodine, in analogy to the decomposition of SPI_3 .^[9] To prove this hypothesis we repeated the reaction of OPCl_3 with LiI in CDCl_3 in a sealed NMR tube with ultrasonic enhancement for 12 h at about 30°C . After 12 h the reaction mixture had turned dark red over some colorless precipitate. The ^{31}P NMR spectrum of this sample only showed one line at $\delta = +173$ ppm, close but not identical to the position of pure PI_3 in the same solvent ($+175$ ppm), but identical to that of a 1:1 mixture of PI_3 and I_2 in CDCl_3 .^[11] This shift of a PI_3 and I_2 mixture was also reported in $\text{CS}_2/\text{C}_6\text{D}_6$.^[12]

We also prepared an equimolar mixture of I_2 and PI_3 , and this mixture has a sharp melting point of $50\text{--}52^\circ\text{C}$. This is close to the cited melting point of OPI_3 at 53°C . Repeating the above NMR-scale reaction in CDCl_3 in a low-temperature ultrasonic bath at -78°C showed the first product detectable in the low-temperature ^{31}P NMR spectrum at 200 K to be P_2I_4 ($\delta(^{31}\text{P}) = 106$ ppm). Continuing the reaction at 0°C , the next detected products were the PI_3/I_2 mixture at $\delta = 173$ ppm, as well as two weak and broad signals at $\delta = -68$ and -167 ppm plus a weak but sharp signal at $\delta = -110$ ppm (Supporting Information). The last signal may well be due to OPCl_2I (cf. SPCl_2I : $\delta(^{31}\text{P}) = -111.5$ ppm); the origin of the broad signals is unclear.

We repeated the reaction of OPCl_3 and LiI on a preparative scale and separated the colorless insoluble precipitate

from the CHCl_3 -soluble fraction. The weights of the soluble and insoluble fractions are in agreement with Equation (2).^[13] The ^7Li and ^{31}P NMR spectra of the insoluble material in D_2O showed the presence of solvated Li^+_{aq} and deuterated orthophosphoric acids (Supporting Information). The IR spectrum of the colorless insoluble material showed it to be P^{V} oxide. The dark red soluble material was shown by Raman spectroscopy to consist of PI_3 and I_2 .^[14]

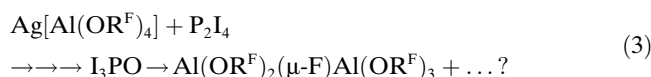
We therefore conclude that the formation of OPI_3 in these mixtures is not detectable by NMR spectroscopy. Therefore, OPI_3 may only be a short-lived intermediate formed by the action of LiI on OPCl_3 . The OPI_3 intermediate appears to disproportionate immediately with formation of P^{V} oxide, I_2 , and PI_3 [Eqs. (1) and (2)]; the P^{V} oxide is included in Eq. (2) as P_4O_{10} .



To back up this conclusion we fully optimized the geometries of all species in Equation (2) at the (RI-)MP2/TZVPP level and assessed the underlying thermochemistry. Equation (2) is exothermic (exergonic) in the gas phase by -7 (-18) kJ mol^{-1} but also when solvation energies are included ($\Delta_r G^\circ_{\text{CHCl}_3} = -17$ kJ mol^{-1} ; COSMO solvation model). By contrast, the MP2/TZVPP calculations show that Equation (2) for the analogous disproportionation reaction of OPBr_3 is endothermic (endergonic) in the gas phase [$\Delta_r H^\circ$ ($\Delta_r G^\circ$) = 47 (35) kJ mol^{-1}] and in solution ($\Delta_r G^\circ_{\text{CHCl}_3} = 35$ kJ mol^{-1}). This is in good agreement with the known solution stability of OPBr_3 but apparent instability of OPI_3 . Thus, in our hands it was impossible to reproduce the synthesis of OPI_3 .

Lewis acid stabilized OPX_3 ($X = \text{Br}, \text{I}$): This led to the question how an OPI_3 -containing species could be stabilized in condensed phases. It appears that P-I bonds in a P^{V} species are more stable in the presence of a positive charge (e.g., PI_4^+ , RPI_3^+).^[15-18] An equivalent to the positive charge would be a strong Lewis acid that coordinates to the oxygen atom and thus prevents disproportionation.

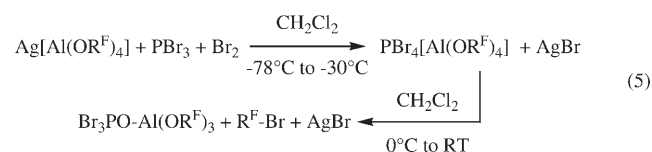
While investigating the chemistry of P_2I_4 and $\text{Ag}[\text{Al}(\text{OR}^{\text{F}})_4]$ ($\text{R}^{\text{F}} = \text{C}(\text{CF}_3)_3$) we realized that the ^{31}P NMR spectra always contained lines at $\delta = -332$ and -337 ppm, where one would expect signals for an OPI_3 -containing molecule. After one reaction [Eq. (3)] we found yellow transparent crystals in a sealed NMR tube containing the reaction mixture that had stood for months at room temperature. We mounted the crystals on an X-ray diffractometer, and all tested crystals (ca. 10) showed the same unit cell. A complete data set of one of the single crystals was recorded and showed them to be the Lewis acid stabilized I_3PO adduct $\text{I}_3\text{PO} \rightarrow \text{Al}(\text{OR}^{\text{F}})_2(\mu\text{-F})\text{Al}(\text{OR}^{\text{F}})_3$ [**1**; Eq. (3)].^[19]



However, we have previously shown by low-temperature ³¹P NMR spectroscopy of in situ reactions^[16] that the initial products of Equation (3) are P₂I₅⁺ (80%) and P₃I₆⁺ (20%). In the course of this reaction, the [Al(OR^F)₄]⁻ ion decomposed and P₂I₅⁺[(R^FO)₃Al(μ-F)Al(OR^F)₃]⁻ formed in 70% yield based on Al.^[16] Thus, it appears likely that the long-term formation of I₃PO→Al(OR^F)₂(μ-F)Al(OR^F)₃ is connected to the reaction of P₂I₅⁺ (or a cation related thereto) with the fluoride-bridged [(R^FO)₃Al(μ-F)Al(OR^F)₃]⁻ ion. Since P₂I₅⁺ disproportionates^[16] over time into PI₄⁺ and P₃I₆⁺ [Eq. (4)], we suspected that PI₄⁺ is the cation responsible for the final transformation as in Equation (3). Therefore, we investigated the reaction of PX₄⁺ (X=Br, I) with the [Al(OR^F)₄]⁻ ion in more detail.

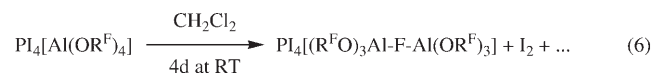


Thus, if one treats Ag⁺[Al(OR^F)₄]⁻ with PBr₃ and Br₂ at -78°C with further stirring at -30°C, one isolates PBr₄⁺[Al(OR^F)₄]⁻ in about 69% yield.^[16] However, if one continues to stir the mixture overnight at room temperature, a quantitative yield of the adduct Br₃PO→Al(OR^F)₃ (**2**) is formed. Similarly, dissolved PBr₄⁺[Al(OR^F)₄]⁻ at temperatures above 0°C is transformed into **2** [Eq. (5)].



Equation (5) is credible, since the phosphorus pentahalides PX₅ (X=Cl, Br) are known to convert alcohols to the corresponding halides.^[20] An in situ NMR investigation of the decomposition of pure PBr₄⁺[Al(OR^F)₄]⁻ in CD₂Cl₂ according to the second part of Equation (2) revealed that this reaction is clean with no by-products other than those shown (¹⁹F, ³¹P, ²⁷Al, ¹³C NMR spectroscopy).

The reaction of PI₄⁺[Al(OR^F)₄]⁻, however, furnished different results: after stirring a CH₂Cl₂ solution of PI₄⁺[Al(OR^F)₄]⁻ for four days at room temperature and subsequent cooling to -25°C, we isolated two fractions of crystals: initially dark I₂ (unit-cell determination, Raman) and, after a second filtration and further concentration, orange PI₄⁺[(R^FO)₃Al(μ-F)Al(OR^F)₃]⁻ [**3**; 74% yield based on Al; Eq. (6)]:^[21]



Compound **3** was independently obtained from Ag⁺[(R^FO)₃Al(μ-F)Al(OR^F)₃]⁻, PI₃, and I₂. Several samples of PI₄⁺[Al(OR^F)₄]⁻ were decomposed in situ in NMR-scale re-

actions with varying conditions from strictly at 0°C, to room temperature, with and without exposure to UV light, and/or ultrasound exposure with increasing temperatures up to 50°C. From the ³¹P NMR spectra of these in situ reactions we noted the following:

- 1) PI₄⁺ was always detectable, but in the course of the reaction the very sharp signal of pure PI₄⁺[Al(OR^F)₄]⁻ at δ(³¹P) = -494 ppm became very broad and gradually shifted to about δ = -460 ppm at the end. This observation is in agreement with the involvement of the PI₄⁺ ion in dynamic exchange (with PI₃?).^[16]
- 2) When the sample was always left at temperatures not exceeding 0°C, we noted only minor formation of one additional sharp ³¹P NMR signal at δ = -337 ppm. In all other cases, a second signal at δ = -332 ppm also formed with about 1/3 of the intensity (Supporting Information).

We assign the two minor signals to I₃PO→Al(OR^F)₃ (δ = -337 ppm) and I₃PO→Al(OR^F)₂(μ-F)Al(OR^F)₃ (δ = -332 ppm). Since Al(OR^F)₃ should be a slightly weaker Lewis acid than Al(OR^F)₂(μ-F)Al(OR^F)₃ and the signal at δ = -337 ppm already appears at 0°C, this assignment appears likely. Overall one can state that PI₄⁺[Al(OR^F)₄]⁻ decomposes at room temperature mainly to give PI₄⁺[(R^FO)₃Al(μ-F)Al(OR^F)₃]⁻, but by a minor path I₃PO→Al(OR^F)₃ and I₃PO→Al(OR^F)₂(μ-F)Al(OR^F)₃ are also formed.

Crystal structures

I₃PO→Al(OR^F)₂-F-Al(OR^F)₃ (**1**) and Br₃PO→Al(OR^F)₃ (**2**): The overall geometry of I₃PO→Al(OR^F)₂(μ-F)Al(OR^F)₃ (**1**) in Figure 1 is reminiscent of that of the [(R^FO)₃Al(μ-F)Al(OR^F)₃]⁻ ion in which one anionic OR^{F-} ligand is replaced by the neutral OPI₃ molecule. The geometry around the phosphorus atom is almost ideally tetrahedral as seen by the small range of the O-P-I and I-P-I bond angles of 109.2(6)–

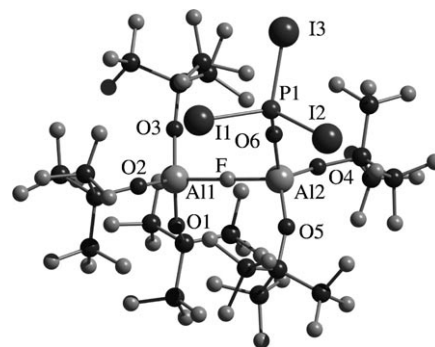


Figure 1. Asymmetric unit of the solid-state structure of **1**. Selected bond lengths [Å] and angles [°]: P1–I1 2.335(3), P1–I2 2.381(3), P1–I3 2.332(3), P1–O1 1.496(7), Al2–O6 1.746(7), Al1–F 1.781(4), Al2–F 1.739(4), Al1–O1 1.687(7), Al1–O2 1.697(7), Al1–O3 1.694(6), Al2–O4 1.674(7), Al2–O5 1.667(6); O6–P1–I1 109.2(2), O6–P1–I2 109.4(2), O6–P1–I3 109.8(2), I3–P1–I1 109.91(9), I3–P1–I2 109.11(9), I1–P1–I2 109.49(9), Al1–F–Al2 179.0(2), C1–O1–Al1 147.3(3), C5–O2–Al1 144.1(5), C9–O3–Al1 155.5(5), C13–O4–Al2 145.6(6), C17–O5–Al2 157.8(5).

109.91(9)°. The P–I bond lengths in **1** are very short and range from 2.332(2) to 2.381(2) Å (av 2.349 Å) and may be compared to those of $\text{PI}_4^+[\text{Al}(\text{OR})_4]^-$ (av 2.370 Å).^[16] The P–O bond length of 1.496(7) Å is about 0.05 Å longer than those of the free OPX_3 (X=F, Cl, Br) molecules (1.436–1.449 Å). The structural parameters of the fluoride-bridged alane unit are similar to those of the $[(\text{R}^{\text{F}}\text{O})_3\text{Al}(\mu\text{-F})\text{Al}(\text{OR}^{\text{F}})_3]^-$ ion.^[16,22–24]

$\text{Br}_3\text{PO} \rightarrow \text{Al}(\text{OR}^{\text{F}})_3$ (**2**) contains tetrahedral OPBr_3 moieties that are coordinated to the $\text{Al}(\text{OR})_3$ Lewis acid (Figure 2). The P–Br distances are short (av 2.098(7) Å)

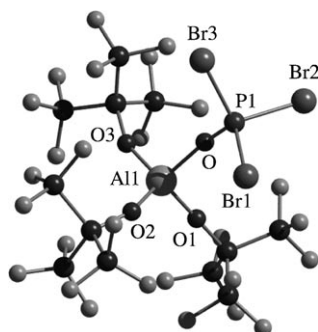


Figure 2. Asymmetric unit of the solid-state structure of **2**. All atoms are drawn as spheres of arbitrary radius. Selected bond lengths [Å] and angles [°]: Br1–P1 2.097(4), Br2–P1 2.097(5), Br3–P1 2.101(5), P1–O 1.465(11), Al1–O2 1.648(11), Al1–O3 1.666(11), Al1–O1 1.686(12), Al1–O 1.788(10); O–P1–Br1 111.1(5), O–P1–Br2 108.2(6), Br1–P1–Br2 108.2(2), O–P1–Br3 113.6(6), Br1–P1–Br3 107.7(2), Br2–P1–Br3 107.9(2), P1–O–Al1 158.7(8).

and, similar to $\text{I}_3\text{PO} \rightarrow \text{Al}(\text{OR}^{\text{F}})_2(\mu\text{-F})\text{Al}(\text{OR}^{\text{F}})_3$, even shorter than those in $\text{PBr}_4^+[\text{Al}(\text{OR}^{\text{F}})_4]^-$ (av 2.111 Å). The dative $\text{Br}_3\text{PO} \rightarrow \text{Al}$ bond in **2** is 0.042 Å longer than that in **1**, just as $\text{Al}(\text{OR}^{\text{F}})_2(\mu\text{-F})\text{Al}(\text{OR}^{\text{F}})_3$ is a stronger Lewis acid than $\text{Al}(\text{OR}^{\text{F}})_3$. In agreement with this, the P–O distance in **2** is 0.031 Å shorter than that in **1**. The structural parameters of the coordinated $\text{Al}(\text{OR}^{\text{F}})_3$ moiety ($d(\text{Al}-\text{O})_{\text{av}} = 1.667(11)$ Å) are normal and resemble those in $[(\text{R}^{\text{F}}\text{O})_3\text{Al}-\text{Al}(\text{OR}^{\text{F}})_3]^-$ and $\text{THF} \rightarrow \text{Al}(\text{OR}^{\text{F}})_3$.^[16,23,24]

$\text{PI}_4^+[\text{Al}(\text{OR}^{\text{F}})_4]^-$ (**4**) and $\text{PI}_4^+[(\text{R}^{\text{F}}\text{O})_3\text{Al}-\text{F}-\text{Al}(\text{OR}^{\text{F}})_3]^-$ (**3**): The structure of **4** is of rather bad quality ($R1 = 13\%$), since the crystals grew within minutes on addition of CS_2 . We mainly see the structure as evidence that $\text{PI}_4^+[\text{Al}(\text{OR}^{\text{F}})_4]^-$ may also crystallize in a less ordered monoclinic phase with $a = 13.669$, $b = 9.684$, $c = 13.959$ Å, $\beta = 91.67^\circ$ at 130 K. By contrast the structure of $\text{PI}_4^+[(\text{R}^{\text{F}}\text{O})_3\text{Al}(\mu\text{-F})\text{Al}(\text{OR}^{\text{F}})_3]^-$ (**3**) is well behaved (Figure 3). Compound **3** consists of well-separated ions of tetrahedral PI_4^+ and $[(\text{R}^{\text{F}}\text{O})_3\text{Al}(\mu\text{-F})\text{Al}(\text{OR}^{\text{F}})_3]^-$ that adopt a distorted CsCl structure (packing dia-

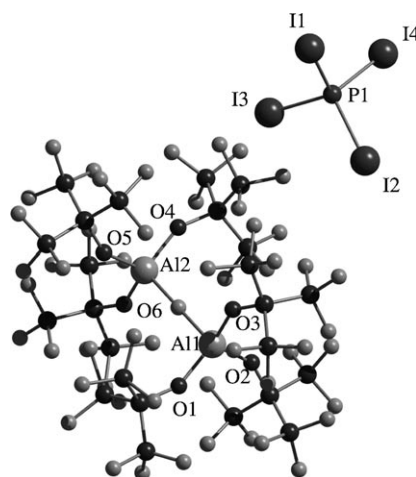


Figure 3. Section of the solid-state structure of **3**. All atoms are drawn as spheres of an arbitrary radius. For clarity, a second PI_4^+ and two $\text{FAl}(\text{OR}^{\text{F}})_3$ with the $(\text{Al})\text{F}$ on a special position are not shown (see Supporting Information). Selected bond lengths [Å] and angles [°]: P1–I1 2.354(3), P1–I3 2.354(3), P1–I2 2.359(3), P1–I4 2.362(2), Al1–O2 1.693(6), Al1–O1 1.698(5), Al1–O3 1.701(7), Al1–F01 1.766(5), Al2–O4 1.692(6), Al2–O6 1.700(7), Al2–O5 1.708(7), Al2–F01 1.772(5); I1–P1–I3 108.72(11), I1–P1–I2 111.03(11), I3–P1–I2 108.73(10), I1–P1–I4 108.29(10), I3–P1–I4 109.36(11), I2–P1–I4 110.68(10).

gram: Supporting Information). The structural parameters of the $[(\text{R}^{\text{F}}\text{O})_3\text{Al}(\mu\text{-F})\text{Al}(\text{OR}^{\text{F}})_3]^-$ anion are normal and resemble those observed earlier.^[16,23,24] The P–I bond lengths of on average 2.357(3) Å are slightly shorter than those in $\text{PI}_4^+[\text{Al}(\text{OR}^{\text{F}})_4]^-$ (2.3700(4) Å)^[16] or $\text{PI}_4^+[\text{AlCl}_4]^-$ (2.368(4) Å) but notably shorter than those in $\text{PI}_4^+[\text{AlI}_4]^-$ (2.396(9) Å)^[25] with a much stronger coordinating counterion.

The solid-state cation–anion contacts exclusively involve F and I atoms; no P–F contact below 3.80 Å was observed. 19 I–F contacts between 3.204 and 3.691 Å, shorter than the sum of the van der Waals radii of 3.70 Å, were found (Supporting Information).

Comparison of free and coordinated OPX_3 : implications for bonding: The structural parameters of all known OPX_3 species (X=F, Cl, Br, I) and their Lewis acid stabilized counterparts are compared in Table 1.

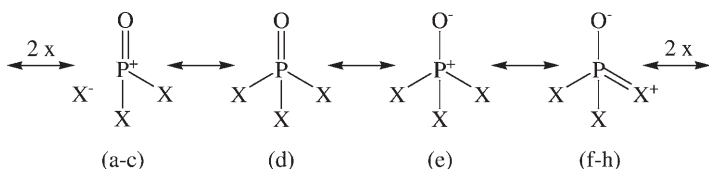
The P–O bond length increases with decreasing electronegativity of the halogen and is at its maximum in free OPI_3

Table 1. Experimental and calculated structural parameters of free and Lewis acid stabilized OPX_3 molecules (X=F–I).

| OPX_3 (exptl) | $d(\text{P}-\text{O})$ [Å] | $d(\text{P}-\text{X})$ [Å] | X–P–X [°] | OPX_3 (calcd, MP2/TZVPP) | $d(\text{P}-\text{O})$ [Å] | $d(\text{P}-\text{X})$ [Å] | X–P–X [°] |
|--|----------------------------|----------------------------|-----------|--|----------------------------|----------------------------|-----------|
| OPF_3 | 1.436 | 1.524 | 101 | OPF_3 | 1.452 | 1.540 | 100.7 |
| OPCl_3 | 1.449 | 2.002 | 106 | OPCl_3 | 1.467 | 2.005 | 103.3 |
| OPBr_3 | 1.44 | 2.16 | 108 | OPBr_3 | 1.472 | 2.183 | 104.0 |
| $\text{Br}_3\text{PO} \rightarrow \text{Al}(\text{OR}^{\text{F}})_3$ | 1.465 | 2.098 | 108.2 | $\text{F}_3\text{Al} \leftarrow \text{OPBr}_3$ | 1.501 | 2.149 | 107.0 |
| OPI_3 | – | – | – | OPI_3 | 1.480 | 2.421 | 105.1 |
| $[\text{Al}]^{\text{al}} \leftarrow \text{OPI}_3$ | 1.496 | 2.349 | 109.5 | $\text{F}_3\text{Al} \leftarrow \text{OPI}_3$ | 1.513 | 2.384 | 108.1 |

[a] $[\text{Al}] = \text{Al}(\text{OR}^{\text{F}})_2(\mu\text{-F})\text{Al}(\text{OR}^{\text{F}})_3$.

(1.480, calcd) and I₃PO→Al(OR^F)₂(μ-F)Al(OR^F)₃ (1.496, X ray). Coordination to a Lewis acid like AlF₃ (calcd) as well as Al(OR^F)₃ and Al(OR^F)₂(μ-F)Al(OR^F)₃ (exptl) further elongates the P–O distances by about 0.03 Å and shortens the P–X bonds by 0.035–0.062 Å. Thus the P–O distances in the adducts **1** and **2** slowly approach values for a P^V–O single bond, for example, 1.60 Å in P₄O₁₀, and the P–X bonds become much shorter than a usual P–X single bond (2.20 Å in PBr₃ or 2.43 Å in PI₃) or even in PX₄⁺ (see above). This is in agreement with the most important OPX₃ Lewis structures in Scheme 1.



Scheme 1. Likely Lewis structures for OPX₃.

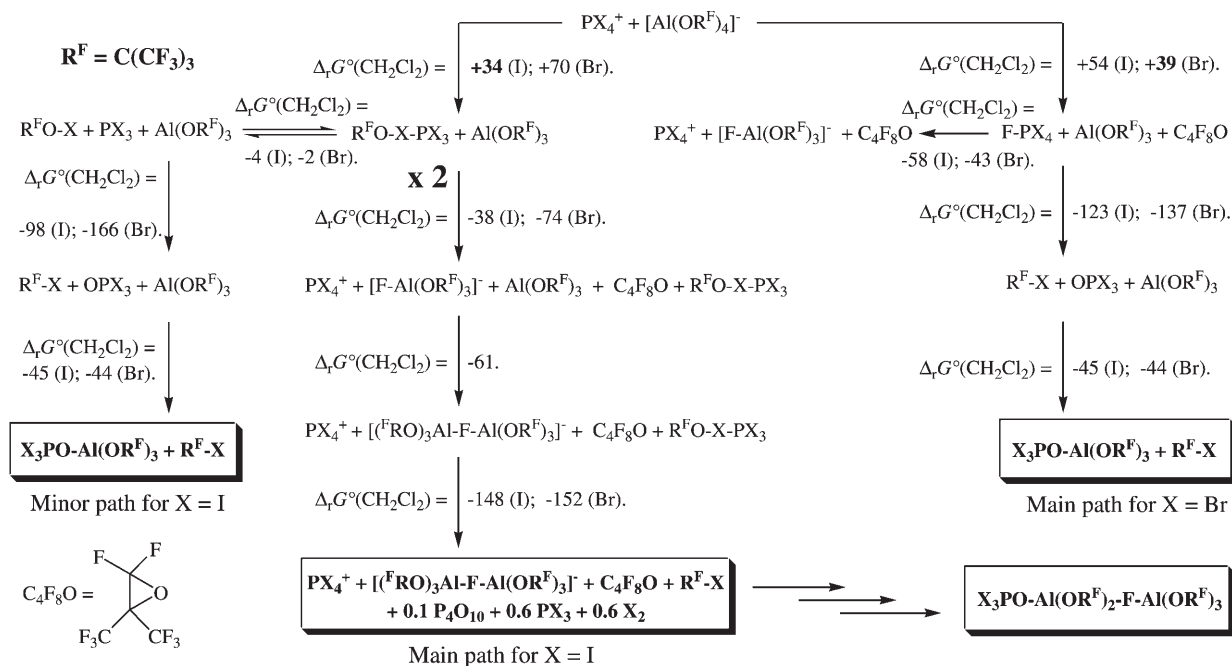
In contrast to the situation for the lighter homologue ONF₃, Lewis structures a–c probably have minor importance for OPX₃ (X = Cl–I). The less electronegative the halogen, the better it can bear a positive partial charge, as in f–h. Thus, for X = Br and I, Lewis structures f–h with a P–O single bond and a P–X bond order of 1.33 have increasing weight that is even greater in the OPX₃ adducts **1** and **2**. In agreement with Lewis structures f–h the halogen atoms of the coordinated OPX₃ molecules exhibit weak intra- and intermolecular solid-state interactions to fluorine atoms of the Lewis acid part (Br: 7 contacts at 3.117–3.398 Å; I: 13 contacts at 3.232–3.673 Å), while the phosphorus atoms show

no fluorine contact below their van der Waals radii of 3.4 Å (Supporting Information). For I₃PO→Al(OR^F)₂(μ-F)Al(OR^F)₃ the number and strengths of I–F contacts per iodine atom are similar to those observed above for the charged PI₄⁺[(R^FO)₃Al(μ-F)Al(OR^F)₃][–] (Supporting Information). Overall the presence of X–F but absence of P–F contacts strongly supports the importance of Lewis structures f–h. In agreement with the lower electronegativity of iodine and thus higher capability to bear positive charge, the number of I–F contacts (13) is larger than the number of contacts to the more electronegative bromine atoms (7).

On the formation of **1** and **2**: mechanistic considerations:

We were surprised that decomposition of PX₄⁺[Al(OR^F)₄][–] proceeds with formation of very different products for X = Br (only Br₃PO→Al(OR^F)₃) and X = I (majority: PI₄⁺[(R^FO)₃Al(μ-F)Al(OR^F)₃][–]; minor components: I₃PO→Al(OR^F)₃ and I₃PO→Al(OR^F)₂(μ-F)Al(OR^F)₃). To understand this observation we optimized compounds which are likely involved in the process by DFT calculations. From these calculations the hypothetical mechanism delineated in Scheme 2 evolved as the most likely. It agrees with all experimental observations.

The main difference between the decomposition for X = I and Br is probably the primary step of anion degradation: According to the analysis of our calculations we propose that for X = I the reaction starts by [OR^F][–] abstraction while that for X = Br starts with F[–] abstraction. After these initial endergonic decomposition steps, the reactions giving the final products are all exergonic (Scheme 2). A decomposition related to the route for X = I was observed for the “PCl₂⁺” intermediate;^[23,36] the decomposition for X = Br is related to the decomposition observed for the [B(CF₃)₄][–]



Scheme 2. Hypothetic mechanism of the formation of Br₃PO→Al(OR^F)₃, PI₄⁺[(R^FO)₃Al(μ-F)Al(OR^F)₃][–], and I₃PO→Al(OR^F)₂(μ-F)Al(OR^F)₃ in agreement with all experimental observations and according to BP86/SV(P) calculations. The calculated Gibbs energies in CH₂Cl₂ are given in kJ mol^{–1}.

anion.^[26] For a detailed analysis and more comments, see Supporting Information.

Conclusion

We have shown that the preparation of OPI₃ from LiI and OPCI₃ does not proceed as indicated in the original paper and that OPI₃ may only be involved as an unobserved intermediate in this process. The final products of this reaction are P^V oxides, PI₃, I₂, and LiCl. The obtained soluble dark red material initially assigned as OPI₃ is a mixture of PI₃ and I₂, as shown by X-ray crystallography, NMR and Raman spectroscopy, melting point, and quantum-chemical calculations. Low-temperature in situ NMR reactions showed that the initial products at -78 °C are P₂I₄ and likely some OPCI₂I. This observation is similar to the reaction of LiI and SPCl₃; pure SPI₃ also remains unknown.^[9] Thus, in our hands it was impossible to verify the existence of free OPI₃ and it appears that the text book entries for OPI₃ should be revised accordingly.

We have presented the first structure of any OPI₃ moiety and assigned ³¹P NMR chemical shifts to these compounds. Starting from PX₄⁺[Al(OR^F)₄]⁻ one can obtain Lewis acid stabilized OPX₃ adducts for X=Br in quantitative yield but for X=I only as minor byproducts in low concentration. The main product of PI₄⁺[Al(OR^F)₄]⁻ decomposition is PI₄⁺[(R^FO)₃Al(μ-F)Al(OR^F)₃]⁻. Formation of OPX₃ from the [Al(OR^F)₄]⁻ ion and PX₄⁺ is in agreement with the common knowledge that phosphorus pentahalides convert alcohols (or alkoxides as in [Al(OR^F)₄]⁻) to the corresponding halides.^[20]

Experimental Section

All manipulations were performed using standard Schlenk or dry box techniques and a dinitrogen or argon atmosphere (H₂O and O₂ < 1 ppm). Apparatus was closed by J. Young valves with a glass stem (leak-tight at -80 °C). All solvents were rigorously dried over P₂O₅, degassed prior to use, and stored under N₂. PBr₃ (Fluka) and X₂ (X=Br, I; Merck) were purchased and purified prior to use by distillation or sublimation. PI₃ was prepared from white phosphorus and iodine in CS₂, and its purity was checked by Raman spectroscopy. M[Al(OR^F)₄] (M=Li, Ag),^[27] Ag⁺[(R^FO)₃Al(μ-F)Al(OR^F)₃]⁻,^[23] and PX₄⁺[Al(OR^F)₄]⁻ (X=Br, I)^[16] were prepared according to the literature. Raman and IR spectra were recorded with a 1064 nm laser on a Bruker IFS 66v spectrometer equipped with the Raman module FRA106 (Karlsruhe) or a Bruker Vertex 70 with the RAM II Raman module (Lausanne). IR spectra were recorded in Nujol mull between CsI plates. NMR spectra of sealed samples were run on a Bruker AC250 spectrometer (Karlsruhe) or Bruker Avance 400 MHz spectrometer (Lausanne) and were referenced to the solvent (¹H, ¹³C) or external H₃PO₄ (³¹P), CFC₃ (¹⁹F), and aqueous AlCl₃ (²⁷Al).

Reaction leading to I₃PO → Al(OR^F)₂(μ-F)Al(OR^F)₃ (1): Ag(CH₂Cl₂)[Al(OR^F)₄] (0.439 g, 0.378 mmol) and P₂I₄ (0.215 g, 0.378 mmol) were weighed into one bulb of a single-piece apparatus. Dichloromethane (ca. 10 mL) was condensed onto the solid mixture at 77 K and the resulting suspension was stirred for 30 min at room temperature. Part of the brownish yellow solution was transferred into an NMR tube, which was stored at -30 °C. After recording the spectra and storage for months at RT a larger quantity of uniform yellow crystals precipitated from this sol-

ution, which were shown to be I₃PO → Al(OR^F)₂(μ-F)Al(OR^F)₃ (1; X-ray). NMR data of the initial solution: ¹³C NMR (63 MHz, CH₂Cl₂/10% CD₂Cl₂, 25 °C): δ = 120.5 ppm (q, CF₃, J_{CF} = 284.4 Hz); ²⁷Al NMR (78 MHz, CH₂Cl₂/10% CD₂Cl₂, 25 °C): δ = 33.8 ppm (s, ν_{1/2} = 213 Hz); ³¹P NMR (101 MHz, CH₂Cl₂/10% CD₂Cl₂, 25 °C): δ = 96.3 (d, ¹J_{PF} = 448 Hz), -58.1 (d, ¹J_{PF} = 442 Hz), -332.4 (s), -336.6 ppm (s).

Reaction leading to Br₃PO → Al(OR^F)₃ (2): Ag(CH₂Cl₂)[Al(OR^F)₄]⁻ (0.558 g, 0.480 mmol) was weighed into a two-bulbed Schlenk vessel connected by a frit plate and closed by valves with a glass stem (J. Young, London). Dichloromethane (3 mL) was condensed onto the mixture at 77 K, and the mixture allowed to reach -78 °C. Then freshly distilled PBr₃ (0.046 mL, 0.480 mmol) and distilled Br₂ (0.025 mL, 0.48 mmol) were added at -78 °C with a Hamilton syringe with a Teflon needle. Immediately, AgBr precipitated. The mixture was allowed to reach room temperature and stirred for another 24 h. Then the yellowish clear solution over off-white precipitate (0.095 g, AgBr) was filtered and all volatiles were removed. The soluble nonvolatile fraction weighed 0.520 g (106% with respect to Br₃PO → Al(OR^F)₃) and according to the ³¹P NMR spectrum contained 95% Br₃PO → Al(OR^F)₃ and 5% undecomposed PBr₄⁺[Al(OR^F)₄]⁻, which accounts for the slightly higher mass balance. The soluble material was recrystallized from CH₂Cl₂ (3 mL) at -25 °C, and all spectroscopic investigations were made on the isolated single crystalline 2.

¹³C NMR (63 MHz, CD₂Cl₂, 25 °C): δ = 122.4 ppm (q, CF₃, J_{CF} = 284.2 Hz); ¹⁹F NMR (CD₂Cl₂, 25 °C): δ = -72.3 ppm (s); ²⁷Al NMR (78 MHz, CD₂Cl₂, 25 °C): δ = 36 ppm (ν_{1/2} = 31 Hz); ³¹P NMR (101 MHz, CD₂Cl₂, 25 °C): δ = -65 ppm; IR: ν(OPBr₃ part) = 1079 (vs, P=O), 483 (m, PBr), 470 cm⁻¹ (m, PBr); ν(Al(OR^F)₃ part) = 1302 (s), 1281 (s), 1260 (vs), 1243 (m), 1220 (ms), 1163 (m), 974 (vs), 801 (vs), 727 (vs), 537 cm⁻¹ (w). Raman: ν(OPBr₃ part) = 480 (24, PBr), 468 (20, PBr), 227 (100, τ-O=PBr₃), 156 (sh, τ-Br₃PO), 141 (55, δ-Br₃PO), 123 cm⁻¹ (4, δ-Br₃PO); elemental analysis calcd (%) for C₁₂Al₁Br₃F₂₇O₄ (1018.75): Br 23.5; found: 24.3.

Reaction leading to PI₄⁺[(R^FO)₃Al(μ-F)Al(OR^F)₃]⁻ (3) as the main product: PI₄⁺[Al(OR^F)₄]⁻ (0.350 g, 0.232 mmol) was weighed into a two-bulbed Schlenk vessel connected by a frit plate and closed by valves with a glass stem (J. Young, London). The compound was dissolved in CH₂Cl₂ (8 mL) and left stirring at room temperature for 5 days. When this solution was cooled to -25 °C dark crystals initially precipitated that were isolated by filtration and shown by X-ray crystallography to be elemental I₂. The filtrate was concentrated to about one half and further cooling at -25 °C yielded orange blocks of PI₄⁺[(R^FO)₃Al(μ-F)Al(OR^F)₃]⁻ (3) in 74% yield with respect to Al (0.174 g). ¹³C NMR (63 MHz, CD₂Cl₂, 25 °C): δ = 120.5 ppm (q, CF₃, J_{CF} = 282.1 Hz); ²⁷Al NMR (78 MHz, CD₂Cl₂, 25 °C): δ = 34 ppm (br, ν_{1/2} = 2400 Hz); ³¹P NMR (101 MHz, CD₂Cl₂, 25 °C): δ = -494 ppm; IR: cation: ν = 404 cm⁻¹ (T₂, PI₄⁺),^[16] anion diagnostics:^[23] ν = 640 (Al(μ-F)Al), 862 cm⁻¹ (AIO); elemental analysis calcd (%) for C₂₄Al₂F₅₅I₆O₆P₁ (2021.73): I 25.1; found: 24.9.

Independent synthesis of PI₄⁺[(R^FO)₃Al(μ-F)Al(OR^F)₃]⁻ (3): Ag⁺[(R^FO)₃Al(μ-F)Al(OR^F)₃]⁻ (0.697 g, 0.338 mmol), PI₃ (0.145 g, 0.349 mmol), and I₂ (0.091 g, 0.359 mmol) were weighed into a two-bulbed Schlenk vessel connected by a frit plate and closed by valves with a glass stem (J. Young, London). Dichloromethane (20 mL) was condensed onto the mixture at 77 K, and the mixture allowed to reach -78 °C with stirring overnight. After stirring for another night at -25 °C, the mixture was filtered and concentrated to about one-half. Overnight orange blocks of PI₄⁺[(R^FO)₃Al(μ-F)Al(OR^F)₃]⁻ crystallized (0.557 g, 66% yield). The analytical data of this material is identical to that given above.

NMR-scale decomposition of PI₄⁺[Al(OR^F)₄]⁻: Six samples of PI₄⁺[Al(OR^F)₄]⁻ (0.100 g, 0.066 mmol) dissolved in CD₂Cl₂ (0.8 mL) and flame sealed in a NMR tube were prepared, and the decomposition was monitored by ³¹P NMR spectroscopy.

X-ray crystal structure determinations: X-ray diffraction data were collected on a STOE IPDS I or IPDS II diffractometer using graphite-monochromated MoK_α (0.71073 Å) radiation. Single crystals were mounted in perfluoroether oil on top of a glass fiber and then brought into the cold stream of a low-temperature device so that the oil solidified. All calcula-

tions were performed on PCs using the Siemens SHELX93 software package. The structures were solved by direct methods and successive interpretation of the difference Fourier maps, followed by least-squares refinement. Crystals of **1** were racemically twinned (ratio 65:35). All atoms were refined anisotropically. Relevant data concerning crystallographic data, data collection, and refinement are compiled in Table 2. CCDC 284884–CCDC-284886 contain the supplementary crystallographic data for this paper. These data can be obtained free of charge from the Cambridge Crystallographic Data Centre via www.ccdc.cam.ac.uk/data_request/cif.

Table 2. Crystallographic and refinement details.

| | 1 | 2 | 3 |
|---|---------------|--|-------------|
| crystal size [mm] | 0.3×0.5×0.5 | 0.2×0.25×0.2 | 0.3×0.3×0.3 |
| crystal system | triclinic | orthorhombic | triclinic |
| space group | <i>P</i> 1 | <i>P</i> 2 ₁ 2 ₁ | <i>P</i> 1̄ |
| <i>a</i> [Å] | 10.384(2) | 21.290(4) | 10.616(2) |
| <i>b</i> [Å] | 10.779(2) | 9.992(2) | 11.867(2) |
| <i>c</i> [Å] | 12.151(2) | 13.551(3) | 41.637(8) |
| α [°] | 96.65(3) | 90 | 83.59(3) |
| β [°] | 105.55(3) | 90 | 86.46(3) |
| γ [°] | 118.50(3) | 90 | 85.42(3) |
| <i>V</i> [Å ³] | 1102.7(4) | 2882.7(10) | 5188.8(18) |
| <i>Z</i> | 1 | 4 | 4 |
| ρ_{calcd} [Mg m ⁻³] | 2.524 | 2.347 | 2.588 |
| μ [mm ⁻¹] | 2.435 | 4.482 | 2.705 |
| abs. correction | numerical | numerical | numerical |
| max/min trans. | 0.4575/0.6540 | 0.531/0.692 | 0.475/0.594 |
| 2 θ [°] | 46.5 | 44.5 | 52.1 |
| <i>T</i> [K] | 160 | 200 | 130 |
| reflns collected | 11392 | 5501 | 20850 |
| reflns unique | 5774 | 3246 | 13992 |
| <i>R</i> (int.) | 0.0637 | 0.0664 | 0.0479 |
| no. of variables | 714 | 472 | 1743 |
| GOF | 1.058 | 0.981 | 1.035 |
| final <i>R</i> (4 σ) | 0.0664 | 0.0793 | 0.0591 |
| final <i>wR</i> 2 | 0.1737 | 0.1871 | 0.1537 |
| largest residual peak [e Å ⁻³] | 0.762 | 0.614 | 1.215 |

Computational details: All calculations were performed with the program TURBOMOLE.^[28,29] The geometries of all species were fully optimized at the (RI-)BP86/SV(P) (DFT) level,^[30] and selected compounds also at the (RI-)MP2 level with triple- ζ valence polarization (two d and one f functions) TZVPP basis set.^[31–33] The 46-electron core of I was replaced by a quasirelativistic effective core potential.^[34] Approximate solvation energies (CHCl₃ solution with $\epsilon_r=4.8$, 298 K) were calculated with the COSMO model^[35] at the (RI-)BP86/SV(P) (DFT) level. Frequency calculations were performed for all species with the module AOFORCE at the (RI-)BP86/SV(P) level, and structures represent true minima without imaginary frequencies on the respective hypersurface. For thermodynamic calculations the zero-point energy and thermal contributions to the enthalpy and the free energy at 298 K were included. The thermal contributions to the enthalpy and entropic contributions to the free energy were calculated with TURBOMOLE using the FreeH module. Optimized geometries of [Al(OR^F)₄]⁻, [(R^FO)₃Al(μ -F)Al(OR^F)₃]⁻, [FAl(OR^F)₃]⁻, Al(OR^F)₃, Br₂, I₂, and C₄F₈O (R^F=C(CF₃)₃) were taken from earlier work.^[16] Machine-readable xyz orientations of the newly calculated structures, the calculated vibrational frequencies, and tables with all contributions to the Gibbs energies are deposited in the Supporting Information.

Acknowledgement

This work was supported by the Deutsche Forschungsgemeinschaft, the Fonds der Chemischen Industrie, the Universität Karlsruhe, and the EPF Lausanne.

- [1] V. G. Kostina, N. G. Feshchenko, A. V. Kirsanov, *Zhl. Obs. Khim.* **1973**, *43*, 209.
- [2] A. W. Allaf, *Spectrochim. Acta A* **1998**, *54*, 921–926.
- [3] The original publication in ref. [1] cites a decomposition temperature of about 200 °C.
- [4] E. G. Robertson, D. McNaughton, *J. Phys. Chem. A* **2003**, *107*, 642–650.
- [5] I. B. Sladkov, *Zh. Prikl. Khim.* **1994**, *67*, 1986–1989.
- [6] G. Dittmer, U. Niemann, *Philips J. Res.* **1982**, *37*, 1–30.
- [7] S. H. Graham, *US Patent USXXAM US 3748520* 19730724, **1973**.
- [8] M. Baudler, G. Fricke, K. Fichtner, *Z. Anorg. Allg. Chem.* **1964**, *327*, 124–127.
- [9] K. B. Dillon, M. d. G. C. Dillon, T. C. Waddington, *Inorg. Nucl. Chem. Lett.* **1977**, *13*, 349–353.
- [10] M. Baudler, G. Fricke, *Z. Anorg. Allg. Chem.* **1963**, *319*, 211–229.
- [11] UV/Vis spectroscopy of this CS₂/C₆D₆ solution revealed the presence of free iodine. To confirm the assumption that an equimolar mixture of PI₃ and I₂ would also give a single resonance at $\delta=+173$ ppm in CDCl₃ we prepared such a sample and indeed found a single line at $\delta=173$ ppm.
- [12] W.-W. du Mont, V. Stenzel, J. Jeske, P. G. Jones, A. Sebald, S. Pohl, W. Saak, M. Baetcher, *Inorg. Chem.* **1994**, *33*, 1502–1505.
- [13] P^V oxide is insoluble and remains with LiCl. Thus the weight of all insoluble (P^V oxide and LiCl) and all soluble material (PI₃ and I₂) was determined. The weights of the soluble and insoluble fraction are in agreement with the stoichiometry of the decomposition given in Equation (2).
- [14] From the concentrated dark red CHCl₃ solution at –30 °C we also obtained orange-red clear crystals which were shown by Raman spectroscopy and an X-ray single-crystal structure determination to be PI₃.
- [15] M. Kaupp, C. Aubauer, G. Engelhardt, T. M. Klapötke, O. L. Malkina, *J. Chem. Phys.* **1999**, *110*, 3897–3902.
- [16] M. Gansior, I. Krossing, L. Müller, I. Raabe, M. Jansen, L. Van Wüllen, *Chem. Eur. J.* **2002**, *8*, 4475–4492.
- [17] I. Tornieporth-Oetting, T. Klapötke, *J. Chem. Soc. Chem. Commun.* **1990**, 132–133.
- [18] W. W. du Mont, F. Ruthe, *Coord. Chem. Rev.* **1999**, *189*, 101–133.
- [19] In the ³¹P NMR spectrum (RT and –70 °C) of the NMR-tube reaction mixture in which later the crystals of **1** grew, recorded after two days of reaction, the following resonances were observed: sharp singlets at $\delta(^{31}\text{P})=-332$ and -337 ppm (probably I₃PO adducts; cf. SP(Br)I₂: $\delta=-315$ ppm) and two unassigned doublets at $\delta(^{31}\text{P})=96.3$ and -58.1 ppm (¹*J*_{PP}=444 Hz).
- [20] G. Cainelli, M. Contento, F. Manescalchi, L. Plessi, *Synthesis* **1983**, *4*, 306–308.
- [21] If CH₂Cl₂ in the decomposition reaction [Eq. (6)] was replaced by a 3:1 CH₂Cl₂:CS₂ mixture at room temperature, within minutes orange crystals formed that were shown by X-ray crystallography to be PI₄⁺[Al(OR^F)₄]⁻ but in another monoclinic modification (the published structure is tetragonal).

- [22] However, some differences occur: The shorter Al–O bond lengths start at the presumably more electrophilic Al2 (1.667–1.674(7) Å; Al1: 1.687–1.697(7) Å) and the almost linear fluoride bridge (Al–F–Al 179.0(2)°) is unsymmetrical by 0.042 Å; the shorter bond points to Al2. On average ($d(\text{Al–O})_{\text{av}}=1.677$ Å, $\angle(\text{C–O–Al})_{\text{av}}=150.1^\circ$) the structural parameters of **1** fit well to those observed for the (RO)₃Al(μ-F)Al(OR)₃[–] anion ($d(\text{Al–F})=1.758$ – 1.770 Å, $d(\text{Al–O})=1.671$ – 1.716 Å).
- [23] A. Bihlmeier, M. Gonsior, I. Raabe, N. Trapp, I. Krossing, *Chem. Eur. J.* **2004**, *10*, 5041–5051.
- [24] I. Krossing, *J. Chem. Soc. Dalton Trans.* **2002**, 500–512.
- [25] S. Pohl, *Z. Anorg. Allg. Chem.* **1983**, *498*, 15–19.
- [26] M. Finze, E. Bernhardt, M. Zehres, H. Willner, *Inorg. Chem.* **2004**, *43*, 490–505.
- [27] I. Krossing, *Chem. Eur. J.* **2001**, *7*, 490–502.
- [28] M. von Arnim, R. Ahlrichs, *J. Chem. Phys.* **1999**, *111*, 9183.
- [29] R. Ahlrichs, M. Bär, M. Häser, H. Horn, C. Kölmel, *Chem. Phys. Lett.* **1989**, *162*, 165.
- [30] K. Eichkorn, O. Treutler, H. Oehm, M. Häser, R. Ahlrichs, *Chem. Phys. Lett.* **1995**, *242*, 652–660.
- [31] F. Weigend, M. Häser, *Theor. Chim. Acta* **1997**, *97*, 331.
- [32] A. Schäfer, C. Huber, R. Ahlrichs, *J. Chem. Phys.* **1994**, *100*, 5829.
- [33] A. Schäfer, H. Horn, R. Ahlrichs, *J. Chem. Phys.* **1992**, *97*, 2571.
- [34] W. Kuechle, M. Dolg, H. Stoll, H. Preuss, *Mol. Phys.* **1991**, *74*, 1245.
- [35] A. Klamt, G. Schürmann, *J. Chem. Soc. Perkin. Trans.* **1993**, *2*, 799.
- [36] In this case we observed the formation of ROPCl₂ in the low-temperature in situ NMR spectrum as a dectet.

Received: September 27, 2005

Revised: February 1, 2006

Published online: May 23, 2006